REGULAR ARTICLE

blood advances

Pirtobrutinib targets BTK C481S in ibrutinib-resistant CLL but second-site BTK mutations lead to resistance

Aishath Naeem,[1,2] Filippo Utro,[3,†] Qing Wang,[4,†] Justin Cha,[2,†] Mauno Vihinen,[5] Stephen Martindale,[1] Yinglu Zhou,[6] Yue Ren,[6] Svitlana Tyekucheva,[6] Annette S. Kim,[7] Stacey M. Fernandes,[1] Gordon Saksena,[2] Kahn Rhrissorrakrai,[3] Chaya Levovitz,[3] Brian P. Danysh,[2] Kara Slowik,[2] Raquel A. Jacobs,[2] Matthew S. Davids,[1,8] James A. Lederer,[9] Rula Zain,[4,10,*] C. I. Edvard Smith,[4,*] Ignaty Leshchiner,[2,*] Laxmi Parida,[3,*] Gad Getz,[2,11,12,*] and Jennifer R. Brown[1,2,8,*]

[1]Department of Medical Oncology, Dana-Farber Cancer Institute, Harvard Medical School, Boston, MA; [2]Cancer Program, Broad Institute of Massachusetts Institute of Technology and Harvard, Cambridge, MA; [3]IBM Research, Yorktown Heights, New York, NY; [4]Department of Laboratory Medicine, Biomolecular and Cellular Medicine, Karolinska Institutet, Karolinska University Hospital Huddinge, SE-141 86, Huddinge, Sweden; [5]Department of Experimental Medical Science, Lund University, SE-221 84, Lund, Sweden; [6]Department of Data Sciences, Dana-Farber Cancer Institute, Harvard T.H. Chan School of Public Health, Harvard University, Boston, MA; [7]Department of Pathology, [8]Department of Medicine, and [9]Department of Surgery, Brigham and Women's Hospital, Boston, MA; [10]Centre for Rare Diseases, Department of Clinical Genetics, Karolinska University Hospital, SE-171 76, Stockholm, Sweden; [11]Department of Pathology, Harvard Medical School, Boston, MA; and [12]Cancer Center and Department of Pathology, Massachusetts General Hospital, Boston, MA

Key Points

- BCR signaling is inhibited by pirtobrutinib in vitro and in vivo regardless of BTK C481S mutation but is reactivated in vivo at progression.
- BTK mutations at the gatekeeper site T474 and second-site kinase-dead mutations lead to resistance to pirtobrutinib.

Covalent inhibitors of Bruton tyrosine kinase (BTK) have transformed the therapy of chronic lymphocytic leukemia (CLL), but continuous therapy has been complicated by the development of resistance. The most common resistance mechanism in patients whose disease progresses on covalent BTK inhibitors (BTKis) is a mutation in the BTK 481 cysteine residue to which the inhibitors bind covalently. Pirtobrutinib is a highly selective, noncovalent BTKi with substantial clinical activity in patients whose disease has progressed on covalent BTKi, regardless of *BTK* mutation status. Using in vitro ibrutinib-resistant models and cells from patients with CLL, we show that pirtobrutinib potently inhibits BTK-mediated functions including B-cell receptor (BCR) signaling, cell viability, and CCL3/CCL4 chemokine production in both BTK wild-type and C481S mutant CLL cells. We demonstrate that primary CLL cells from responding patients on the pirtobrutinib trial show reduced BCR signaling, cell survival, and CCL3/CCL4 chemokine secretion. At time of progression, these primary CLL cells show increasing resistance to pirtobrutinib in signaling inhibition, cell viability, and cytokine production. We employed longitudinal whole-exome sequencing on 2 patients whose disease progressed on pirtobrutinib and identified selection of alternative-site *BTK* mutations, providing clinical evidence that secondary *BTK* mutations lead to resistance to noncovalent BTKis.

Introduction

Covalent Bruton tyrosine kinase (BTK) inhibitors (BTKis) revolutionized the treatment landscape of chronic lymphocytic leukemia (CLL). However, most patients who remain on therapy develop resistance,

Submitted 27 June 2022; accepted 9 October 2022; prepublished online on *Blood Advances* First Edition 26 October 2022; final version published online 9 May 2023. https://doi.org/10.1182/bloodadvances.2022008447.

*R.Z., C.I.E.S., I.L., L.P., G.G., and J.R.B. contributed equally to this study.

†F.U., Q.W., and J.C. contributed equally to this study.

Data are available on request from corresponding author, Jennifer R. Brown (jennifer_brown@dfci.harvard.edu).

The full-text version of this article contains a data supplement.

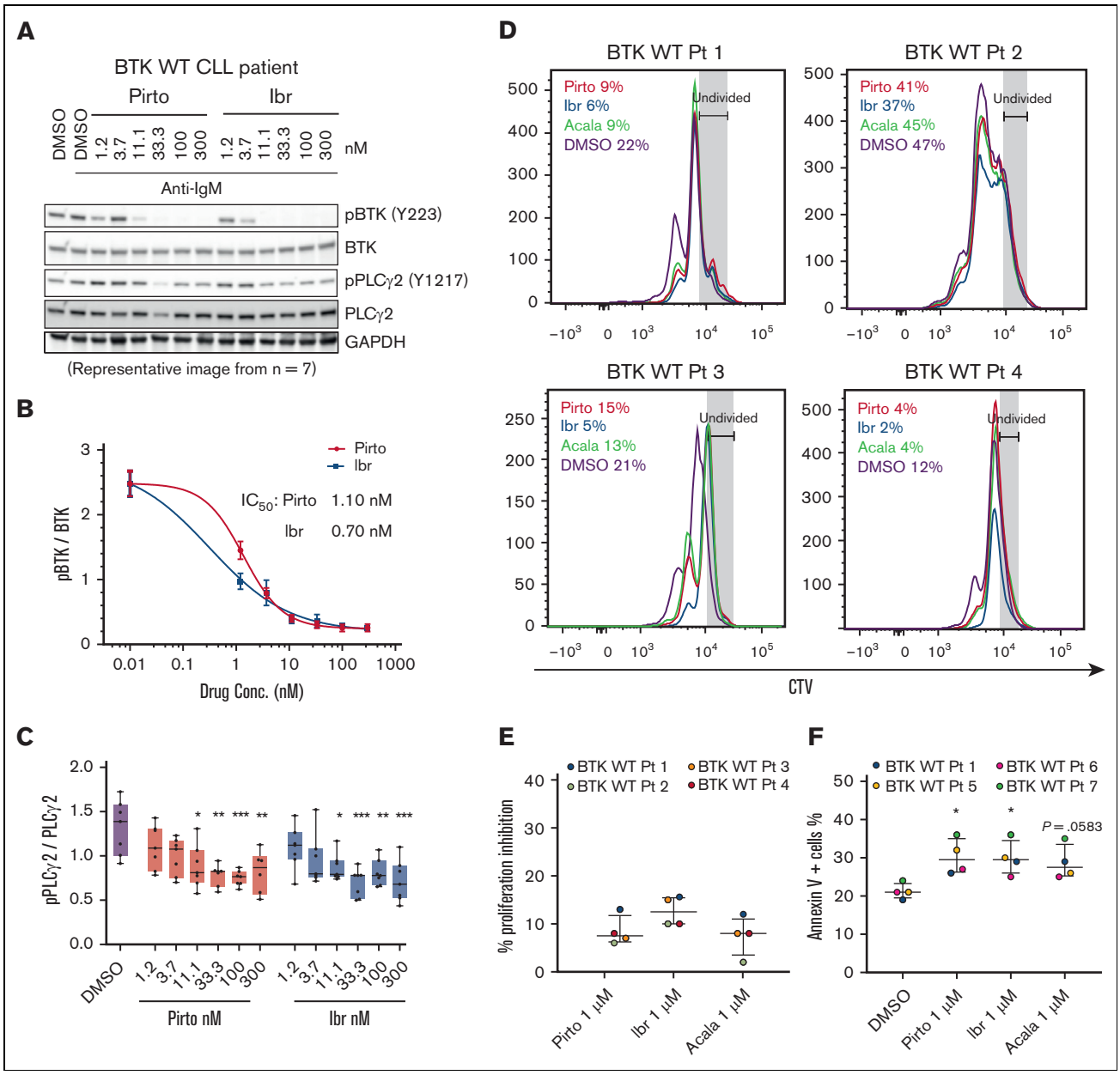

Figure 1. Pirtobrutinib reduced BCR signaling and induced apoptosis in cells from patients with BTK WT CLL. (A-C) BTK WT CLL cells were treated with either pirtobrutinib or ibrutinib with a dose range of 1.2 to 300 nM. Data shown are representative results from n = 7. (A) Representative western blot. (B) BTK Y223 phosphorylation was normalized to total BTK and IC_{50} values were calculated using a 4-parameter fit in GraphPad Prism 9.3 software. (C) Densitometry plots for phospho-PLCγ2 (Y1217), normalized to total PLCγ2. Boxes represent median values with the first and third quartiles; whiskers represent the maximum and minimum values. *P* values shown are for drug vs dimethyl sulfoxide (control). $^{*}P \leq .05$, $^{**}P \leq .01$, and $^{***}P \leq .001$ by mixed effect analysis of variance, Holm-Šidák test. (D-E) CellTrace Violet–labeled BTK WT CLL cells from patients with CLL were incubated with growth stimulants as indicated in "Methods" and treated with 1 μM of either pirtobrutinib, ibrutinib, or acalabrutinib, and cell proliferation was assayed by flow cytometry after a 10-day culture. (D) Histograms showing CTV profiles of 4 patients with BTK WT. Divided cells as a percent of total cells are automatically calculated by the FlowJo software and included in the upper left of each panel. (E) Inhibition of CLL cell proliferation by the indicated drug treatment, normalized to dimethyl sulfoxide, based on data in panel D. (F) Cells from patients with BTK WT CLL were treated with 1 μM of either pirtobrutinib, ibrutinib, or acalabrutinib for 48 hours. Apoptosis was measured with Annexin V propidium iodide staining. Statistics were performed by one-way analysis of variance with Dunnett posttest; $^{*}P \leq .05$. Graphs generated using GraphPad Prism software version 9.3. The data points for panels E and F are color coded by patient. Acala, acalabrutinib; Conc., concentration; CTV, CellTrace Violet; DMSO, dimethyl sulfoxide; GAPDH, glyceraldehyde-3-phosphate dehydrogenase; Ibr, ibrutinib; IgM, immunoglobulin M; Pirto, pirtobrutinib; Pt, patient.

most commonly (50%-75%) from substitution of Cys481 by Ser at the adenosine triphosphate–binding pocket of BTK, thereby abrogating covalent binding of irreversible BTKis.[1-4] Other less common substitutions at this same site (p.C481R/F/Y/G), and gain-of-function mutations in *PLCγ2*, occur at lower frequency than p.C481S but also confer resistance to covalent BTKis.[5-8]

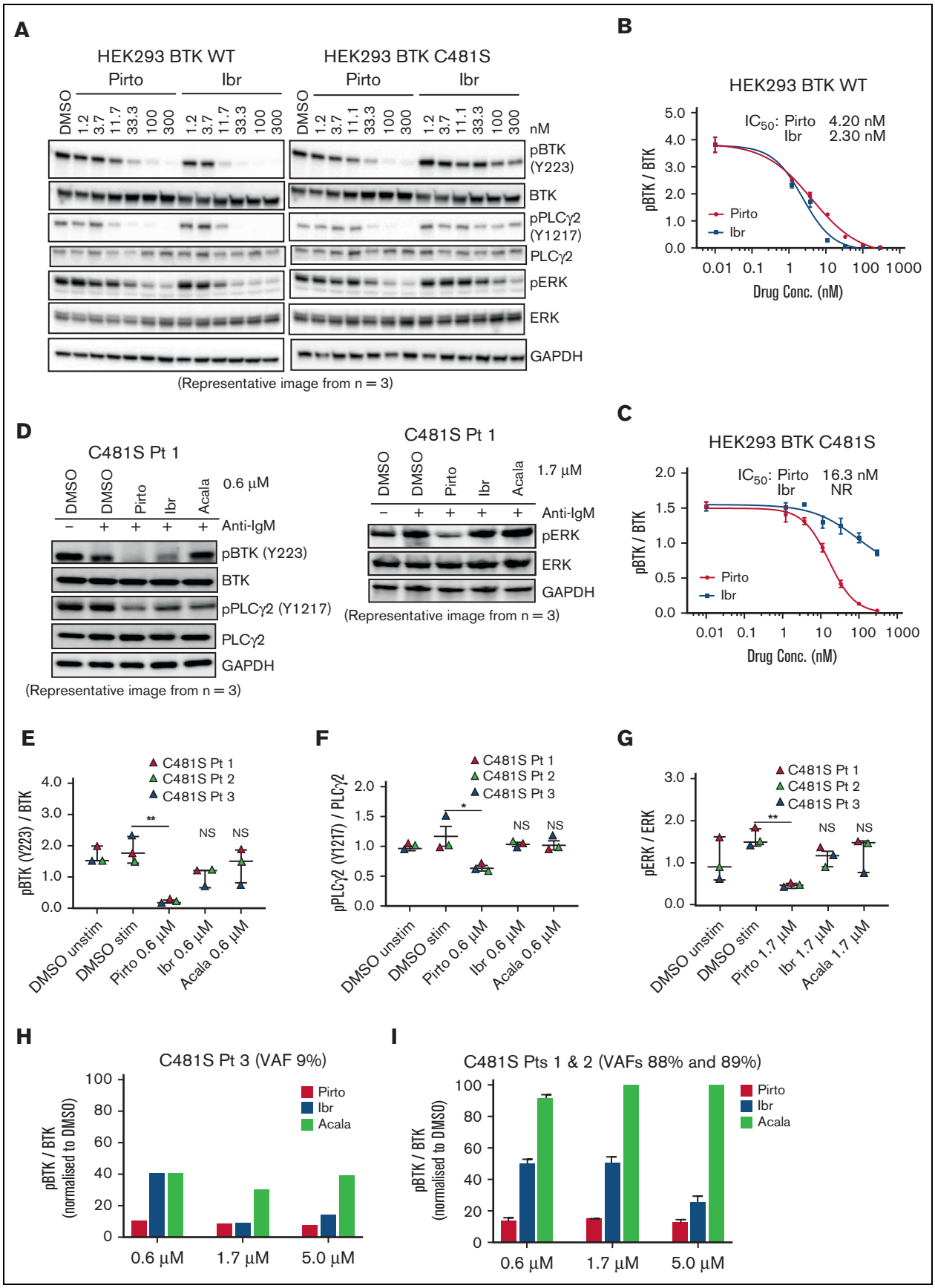

Figure 2.

Reversible or noncovalent BTKis have been developed to inhibit BTK regardless of C481S mutation and offer a therapeutic alternative for patients who have experienced covalent BTKi treatment failure.[9,10] Noncovalent BTKis do not require binding to C481, and they are designed to maintain activity against both wild-type (WT) and C481 mutations. Noncovalent BTKis such as XMU-MP-3, CGI-1746, fenebrutinib (GDC-0853), and nemtabrutinib (Arq-531/MK-1026) have demonstrated potent activity against both WT and C481S BTK in preclinical studies.[11-14] Nemtabrutinib and pirtobrutinib (LOXO-305) are currently in clinical trials in B-cell malignancies and have demonstrated excellent antitumor efficacy; pirtobrutinib in particular is very well tolerated.[10,15]

In this study we demonstrate the preclinical efficacy of pirtobrutinib against WT and C481S BTK by evaluating its impact on viability, proliferation, and chemokine production in CLL cells. We further demonstrate that this ex vivo activity of pirtobrutinib declines as patients develop clinical progression. Resistance mechanisms for reversible BTKis are only starting to be described.[16] To investigate molecular mechanisms underlying disease progression, we performed whole-exome sequencing on 2 patients whose disease progressed on pirtobrutinib and show evidence that multiclonal alternative-site *BTK* mutations confer resistance to noncovalent BTKis.

Methods

Clinical samples

Samples were collected from patients enrolled in our CLL tissue bank approved by the Dana-Farber/Harvard Cancer Center Institutional Review Board, and written informed consent was obtained before sample collection. For the patients with disease progression on pirtobrutinib, serial peripheral blood (tumor) and saliva (normal) samples were collected before and at relapse during each successive therapy including pirtobrutinib.

Cell culture and transfections

The B7.10 cell line, which lacks endogenous BTK, was generated from the DT40 chicken lymphoma in T. Kurosaki's laboratory as previously detailed.[17,18] Site-directed mutagenesis was used to generate 6 single and 3 double BTK mutants as described previously.[19,20] Single mutants were T474I, T474L, M477I, C481R, C481S, and L528W; and double mutants were M477I/C481S, M477I/L528W, and C481S/L528W. WT BTK was used as control.

Clonality estimation using ABSOLUTE

Copy number analysis and estimation of tumor purity, ploidy, and cancer cell fraction (CCF) of mutations were determined using the computational method, ABSOLUTE.[21] Phylogenetics and subclonal dynamics associated with resistance were modeled using the PhylogicNDT and Concerti tools.[22-24]

For additional information, please refer to the supplemental Methods.

Results

Pirtobrutinib is cytotoxic and inhibits BCR signaling in cells from patients with CLL

To confirm that pirtobrutinib is active and inhibits the B-cell receptor (BCR) pathway, we first investigated its activity in CLL-like cell lines, MEC1 and OSU-CLL. We compared the effects of pirtobrutinib with the covalent inhibitors ibrutinib and acalabrutinib on cell viability and BCR signaling. All 3 drugs demonstrated similar inhibition of viability with comparable 50% inhibitory concentration (IC_{50}) values and similar inhibitory effects on the BCR pathway (supplemental Figure 1A-D).

To evaluate inhibition of BCR signaling in cells from patients with CLL with WT BTK, we treated the cells with increasing doses of pirtobrutinib and ibrutinib for 1 hour. Ibrutinib has been shown to inhibit phosphorylation of BTK, PLCγ2, and extracellular signal-regulated kinase (ERK).[25] As expected, our data show that ibrutinib inhibits phospho-BTK with an IC_{50} of 0.7 nM. Similarly, pirtobrutinib also potently inhibits phospho-BTK with an IC_{50} of 1.1 nM (Figure 1A-B; supplemental Figure 2). Both drugs also inhibited phosphorylation of PLCγ2, the immediate downstream substrate of BTK, at concentrations as low as 11.1 nM (Figure 1C).

We then evaluated the effect of pirtobrutinib on proliferation of CLL cells. To achieve this, CellTrace Violet–labeled CLL cells were stimulated to proliferate with stimulants and HS-5 stroma coculture, and treated with 1 μM of either pirtobrutinib, ibrutinib, or acalabrutinib for 10 days before assessment of proliferation by flow cytometry. All 3 drugs demonstrated similar inhibitory effects on proliferation (Figure 1D-E; supplemental Figure 3).

We then compared the cytotoxicity of pirtobrutinib with ibrutinib and acalabrutinib in primary CLL cells from patients by exposing the cells to 1 μM drug concentrations. After 48 hours, we observed a significant induction of apoptosis with pirtobrutinib and ibrutinib compared with control (Figure 1F).

Pirtobrutinib inhibits BCR signaling mediated by BTK C481S

Pirtobrutinib was designed to maintain activity despite C481 mutation. To test this, we used an in vitro BTK C481S model of stably transfected HEK293 cells expressing either BTK WT or C481S BTK. Cells were treated with a dose range of 1.2 to 300 nM of either pirtobrutinib or ibrutinib for 2 hours. In BTK

Figure 2. Pirtobrutinib inhibits BCR signaling in a BTK C481S in vitro model and in cells from patients with BTK C481S CLL. (A-C) HEK293 BTK WT and HEK293 BTK C481S cells were treated with either pirtobrutinib or ibrutinib with a dose range of 1.2 to 300 nM for 2 hours. (A) Representative western blot image from 3 independent experiments. BTK Y223 phosphorylation was normalized to total BTK in HEK293 BTK WT (B) and HEK293 BTK C481S (C) cells. IC_{50} values were calculated using a 4-parameter fit in GraphPad Prism software version 9.3. (D-G) Cells from patients with BTK C481S CLL (n = 3) were pretreated with indicated dosages of pirtobrutinib, ibrutinib, or acalabrutinib for 1 hour followed by anti-IgM stimulation (10 μg/mL) for 30 minutes. (D) Representative western blot images. Quantification of phospho-BTK (E), phospho-PLCγ2 (F), and phospho-ERK (G). The data points are color coded by patient. *P* values shown are for drug vs DMSO stimulated (ie, IgM stimulated). Differences assessed using linear mixed effect models. $*P \leq .05$ and $**P \leq .01$. (H,I) Densitometry plots for phospho-BTK normalized to total BTK. Graphs generated using GraphPad Prism software version 9.3. VAF, variant allele frequency.

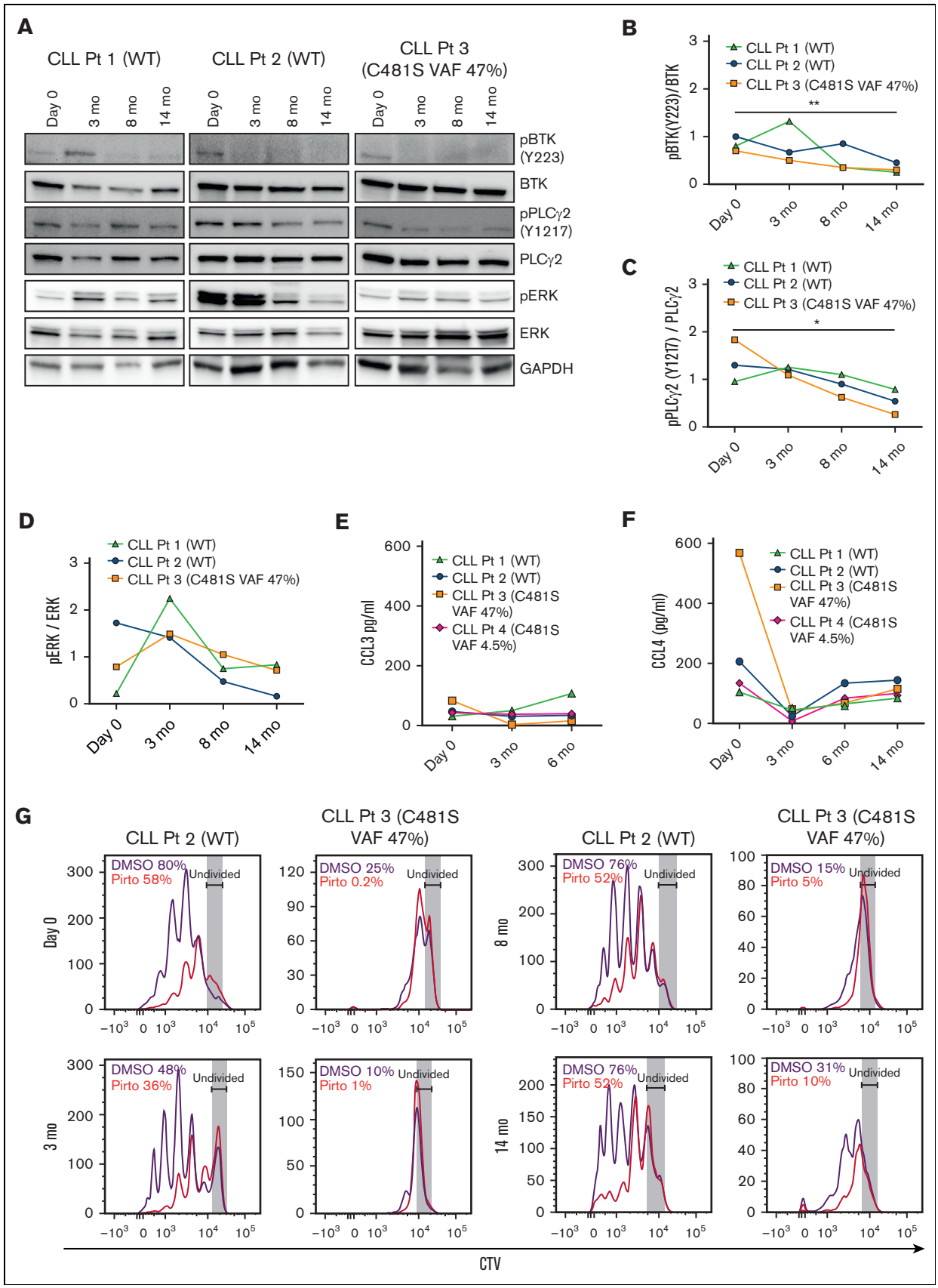

Figure 3.

WT–expressing cells, for both pirtobrutinib and ibrutinib, we observed similar inhibition of phosphorylated BTK (phospho-BTK) at low nanomolar potency, IC_{50} of 4.2 nM and 2.3 nM, respectively; however, against the C481S mutation, ibrutinib lost its efficacy completely whereas pirtobrutinib maintained potency with an IC_{50} of 16 nM (Figure 2A-C; supplemental Figure 4). A similar inhibition pattern was observed in phospho-PLCγ2 with pirtobrutinib maintaining the same inhibition efficiency against both WT and mutant BTK (Figure 2A).

We then treated CLL cells from 3 patients with C481S mutation with 0.6 μM pirtobrutinib, ibrutinib, or acalabrutinib and saw significant decrease in phosphorylation of BTK and PLCγ2 in pirtobrutinib-treated cells. Although phospho-BTK was slightly decreased in ibrutinib-treated cells, the overall inhibitory effect of the covalent BTKi was greatly reduced (Figure 2D-F). Furthermore, we also observed a significant reduction in phosphorylation of the downstream signaling molecule ERK at 1.7 μM of pirtobrutinib, whereas ibrutinib and acalabrutinib showed no significant change (Figure 2D,G). When we grouped the 3 patients with the C481S BTK mutation according to their C481S VAFs, in the patient with a low C481S VAF of 9%, phospho-BTK inhibition with 0.6 μM pirtobrutinib was ≥80%, whereas ibrutinib and acalabrutinib achieved 60% inhibition (Figure 2H). In the other 2 patients with VAFs of 89% and 88%, respectively, at 0.6 μM, pirtobrutinib maintained an inhibitory effect of ≥80% on phospho-BTK. Phospho-BTK inhibition of ibrutinib was only ~50% and acalabrutinib had an inhibitory effect of <10%, consistent with the known lack of acalabrutinib activity against C481S, whereas ibrutinib retains some noncovalent inhibition, particularly at higher concentrations (Figure 2I).[2,26]

Pirtobrutinib is cytotoxic and reduces cytokine secretion in cells from patients with BTK C481S CLL

CCL3 and CCL4 are associated with tumor burden in CLL and have proven to be an excellent biomarker of response to BTKis.[27,28] To evaluate the effect of pirtobrutinib on cytokine secretion, CLL cells from patients with either BTK WT or BTK C481S were treated with 1 μM pirtobrutinib, ibrutinib, or acalabrutinib for 24 hours, and the levels of CCL3 and CCL4 in the supernatants were analyzed by enzyme-linked immunosorbent assay. Although pirtobrutinib, ibrutinib, and acalabrutinib inhibited CCL3 and CCL4 at similar levels in BTK WT cells, only pirtobrutinib significantly inhibited both cytokines in C481S cells (supplemental Figure 5A-B).

Pirtobrutinib inhibits BCR signaling and cytokine secretion and proliferation in responding patients with CLL

We evaluated the effect of pirtobrutinib on BCR signaling and cytokine secretion and proliferation in CLL cells from responding patients currently enrolled in the pirtobrutinib phase 1 trial. We looked at 3 responding patients in total (2 with BTK WT and 1 with BTK C481S). Although phospho-BTK was initially increased in 1 patient with WT BTK at 3 months, densitometry analysis from all 3 patients showed a significant decrease in phospho-BTK and phospho-PLCγ2 at 14 months compared with baseline, irrespective of BTK mutation status (Figure 3A-C). Similarly, although elevated phospho-ERK was observed in cells from 2 patients at 3 months, all 3 patients showed an overall decrease in phospho-ERK in their CLL cells by 14 months (Figure 3D).

All responding patients tested showed steady plasma CCL3 levels across all time points tested (Figure 3E). Similarly, all patients tested maintained CCL4 at low levels up to 14 months (Figure 3F). To assay the effect of pirtobrutinib on proliferation, CellTrace Violet–labeled cells were treated with 1 μM pirtobrutinib, and cell proliferation was assayed by flow cytometry after 10-day culture. We observed steady inhibition of proliferation across all time points in both BTK WT and C481S cells (Figure 3G).

At progression on pirtobrutinib, CLL cells show reactivated BCR signaling, cytokine secretion, and increased cell viability

We looked at 3 patients whose disease progressed during pirtobrutinib therapy and found an increase in BCR signaling pathway activation, as evidenced by increased phosphorylation of BTK, AKT, and ERK at progression (Figure 4A-C). Both CCL3 and CCL4 levels rapidly declined in all 3 patients at 3 months while responding and then sharply increased at progression (Figure 4D-E). Furthermore, the CLL cells from all 3 patients at progression were more resistant to pirtobrutinib in vitro, with significantly less reduction in viability with in vitro drug treatment (Figure 4F).

We further evaluated the effect of pirtobrutinib in vitro, comparing cells from 2 patients at progression vs baseline. At the progression time points, the CLL cells demonstrated reduced induction of apoptosis compared with cells at baseline, after in vitro pirtobrutinib treatment (Figure 4G-H). Similarly, for both patients, cells at progression showed increased resistance to inhibition of proliferation in vitro by pirtobrutinib (Figure 4I-J).

Pirtobrutinib resistance is associated with second-site BTK mutations

For 2 patients whose disease progressed on pirtobrutinib, serial peripheral blood and matched normal samples were collected for whole-exome and RNA sequencing, including before and at relapse on pirtobrutinib (Table 1). One patient with CLL (patient-identifying code, CLL Pt 6) had 16 samples including pretreatment, on-treatment, and at relapse on acalabrutinib, vecabrutinib, and pirtobrutinib (Table 1). The phylogenetic tree shows a truncal clone

Figure 3. Pirtobrutinib inhibits BCR signaling and cytokine secretion and proliferation in responding cells from patients with BTK WT and C481S CLL. (A-D) Proteins were evaluated in defrosted lysates, without in vitro treatment, from cells from 2 patients with BTK WT and 1 patient with BTK C481S CLL, and levels of phospho-BTK, phospho-PLCγ2, and phospho-ERK were analyzed by immunoblotting. (A) Western blots for each patient. (B-D) Densitometry plots for phospho-BTK, phospho-PLCγ2, and phospho-ERK normalized to the corresponding total protein. Differences assessed by analysis of variance followed by Tukey test. (E-F) Plasma CCL3 and CCL4 levels measured by Luminex multiplex assay and enzyme-linked immunosorbent assay, respectively. Graphs generated using GraphPad Prism software version 9.3. Data points in panels B-F are color coded by patient. (G) CellTrace Violet–labeled BTK WT and BTK C481S CLL cells were cocultured with HS-5 green fluorescent protein stroma cells, incubated with growth stimulants as indicated in "Methods" and treated in vitro with 1 μM pirtobrutinib. Cell proliferation was assayed by flow cytometry after a 10-day culture. Divided cells as a percent of total cells are automatically calculated by the FlowJo software and included in the upper left of each panel. $^{*}P \leq .05$ and $^{**}P \leq .01$.

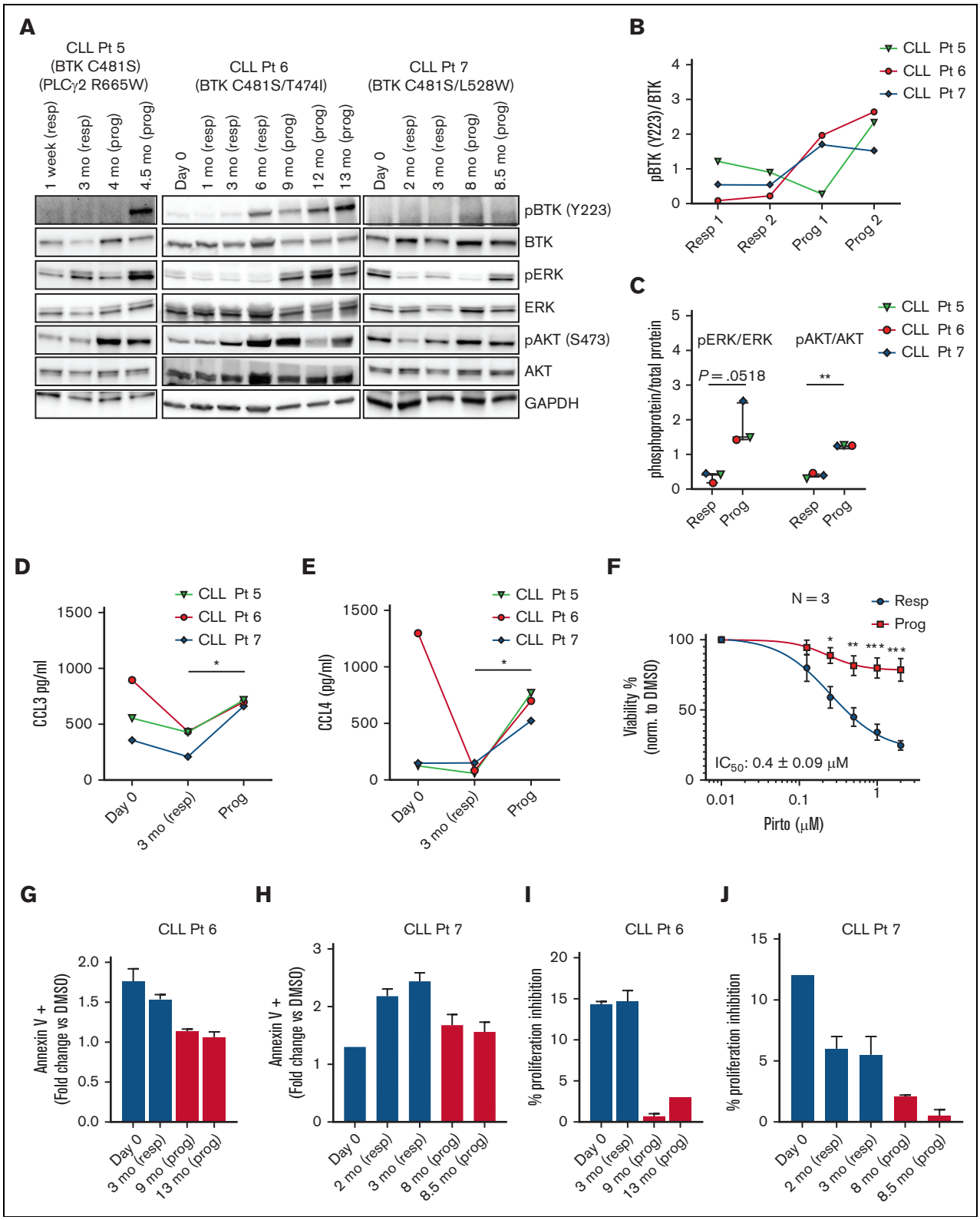

Figure 4. CLL cells from patients with disease progression on pirtobrutinib show increased BCR signaling, increased cytokine secretion, reduced inhibition of proliferation, reduced in vitro cell death, and increased cell viability. (A-J) Primary CLL cells obtained at baseline (day 0), responding, and progression time points during pirtobrutinib treatment were used in the analysis. (A) Western blots of lysates from CLL cells of 3 patients whose disease progressed, looking at total and phospho-BTK, total and phospho-ERK, total and phospho-AKT, and GAPDH without additional in vitro drug treatment. (B-C) Densitometry plots for phospho-BTK, phospho-ERK, and phospho-AKT normalized to the corresponding total protein. (D-E) Plasma CCL3 and CCL4 levels measured by Luminex multiplex assay and enzyme-linked immunosorbent assay, respectively.

(green) in all samples, carrying mutations in known CLL cancer driver genes (Figure 5A-B; supplemental Tables 1 and 3). Clonal analysis of samples during acalabrutinib treatment shows steady selection of a subclone (orange) harboring *BTK* p.C481S mutation, a known mechanism of acalabrutinib resistance, with CCF of 92% (95% confidence interval, 87-98) at relapse. This clone maintained this CCF level during therapy with vecabrutinib, a noncovalent BTKi with lower clinical effectiveness that is no longer in development in CLL,[29] but then steadily decreased during effective therapy with pirtobrutinib. Concerti's time-scaled phylogenetic tree shows the birth of a new clone containing the *BTK* gatekeeper mutation, p.T474I, during acalabrutinib treatment, which then grows rapidly under pirtobrutinib treatment, dominating nearly the entire cancer cell population and replacing the prior p.C481S clone (Figure 5A-C; supplemental Table 5). This complete clonal shift during pirtobrutinib treatment suggests that pirtobrutinib effectively inhibits the p.C481S clone, whereas the p.T474I gatekeeper clone is likely driving resistance in this patient. In support of this, we also observed an additional gatekeeper clone at low CCF, *BTK* p.T474L, as well as another BTK mutation, p.M477I (Figure 5A-C; Table 1). Manual inspection of variant calls using Integrative Genomics Viewer[30] (IGV) showed that *BTK* p.M477I was in *cis* with the dominant p.T474I clone, indicating that they co-occur in the same cells. In contrast, the p.T474L is in *trans* to p.M477I, that is, in different alleles (supplemental Figure 6A). Inspection of RNA sequencing reads on IGV confirmed these resistance mutations in similar clonal proportions to the DNA (supplemental Figure 7A; Table 1). Treatment with pirtobrutinib also led to the development of another subclone from the p.T474I-containing clone, carrying acquired mutations in the known cancer-related genes, *RAC1* and *TP53BP2* (Figure 5A-C; supplemental Table 1).

Another patient with CLL (CLL Pt 7) had 10 samples evaluated before, during, and at relapse on ibrutinib and pirtobrutinib (Table 1). During ibrutinib therapy, we observed a steady increase in a clone (cyan) harboring mutations in known CLL driver genes, *TP53* p.S240G and *SF3B1* p.K666N, reaching CCFs of >40% at relapse on ibrutinib (Figure 5D-E; supplemental Tables 2 and 4). We also noted a significant increase (>25%) in a clone (purple) carrying the *BTK* p.C481R mutation (CCF, 28%) and a 5% increase in a clone (black; CCF, 14%) harboring the mutations *BTK* p.C481S and *TP53* p.R196*. All clones remained roughly stable during chimeric antigen receptor T-cell therapy between ibrutinib and pirtobrutinib. During pirtobrutinib treatment, the purple and black clones in the phylogenetic plot displayed different dynamics, both shifting their CCFs. The purple clone, that harbors *BTK* p.C481R, decreased to a CCF of 15%, whereas the black clone, which carries the *BTK* p.C481S and *TP53* p.R196* mutations, increased its CCF to 31% at relapse on pirtobrutinib (Figure 5D; supplemental Tables 2 and 4). Concerti's phylogenetic tree also captures the birth of a resistant clone harboring *BTK* p.L528W, which increased during pirtobrutinib therapy, reaching a CCF of 30% at time of progression (Figure 5F; supplemental Figure 6B; supplemental Table 6). *BTK* p.L528W has been described as conferring resistance to ibrutinib and zanubrutinib in CLL and has recently been associated with resistance to pirtobrutinib.[16] The rapid increase of *BTK* p.L528W CCF from 2% to 30% with disease progression during pirtobrutinib suggests that *BTK* p.L528W mutation may be contributing to resistance in 1 patient with CLL (CLL Pt 7). Furthermore, this mutation is preferentially expressed in our RNA sequencing data, rising from 1% VAF at pirtobrutinib initiation to 43% at 3 months and 82% at progression (supplemental Figure 7B). This clone also carries a *TP53* p.Q317* at low levels (CCF, 6%), which may also be contributing to disease progression (Figure 5C-F; supplemental Tables 2 and 6).

Docking pirtobrutinib on BTK

We sought to understand pirtobrutinib binding to BTK to understand the effect of these mutations. Covalent and noncovalent BTKis bind predominantly in different orientations. Analysis of residues related to binding distance in the structures indicated that many of the binding residues are still shared, although there are also type-specific interactions.[31] Wang et al reported that pirtobrutinib would bind similarly to ibrutinib.[16] We combined our experimental evidence with that of Wang et al and conclude that pirtobrutinib likely binds in a mode more similar to other noncovalent inhibitors. Our analysis of the binding sites was based on 4 experimental inhibitor structures: 2 covalent (ibrutinib and zanubrutinib) and 2 noncovalent inhibitors (fenebrutinib and RN486).[31] Combined, the 2 studies indicate variations at positions likely to affect pirtobrutinib binding. Wang et al indicated 5 such residues: V416, A428, M437, T474, and L528. M437 has not been found to interact with inhibitors of either class. V416 interacts with ibrutinib but not with the other covalent inhibitor, zanubrutinib, whereas it binds to both noncovalent inhibitors. A428 binds to zanubrutinib and interacts with both noncovalently binding molecules. T474 binds to all 4 investigated inhibitors. L528 binds to 1 representative from each category. Combined, these results suggest that residues that affect pirtobrutinib binding may be in common with other noncovalent inhibitors. When we combine our results for variants M477 and C481, which bind equally well to both types of inhibitors, the binding data support a noncovalent inhibitor binding mode. The likely binding mode was obtained by docking pirtobrutinib to the structure of BTK with CGI-1746. Pirtobrutinib includes highly polar residues, with 3 and 1 fluoride residues, respectively, located at opposite ends of the molecule. The single fluoride group was docked to enable interaction with the CGI-1746 isopropyl group. The opposite end could interact with the sulfhydryl group of C481 and orient the molecule (Figure 6A). Pirtobrutinib is a flexible

Figure 4 (continued) Data points in panels B to E are color coded by patient. (F) CLL cells at responding and progression time points for each of the 3 patients were incubated with indicated doses of pirtobrutinib for 48 hours and effect on viability was analyzed using CellTitre-Glo reagent. Data reported as mean ± standard error of the mean from n = 3. (G-J) Cells were cocultured with HS-5 green fluorescent protein stroma cells. (G-H) Apoptosis was induced by 1 μM pirtobrutinib for 48 hours and analyzed by flow cytometry. (I-J) CTV-labeled cells were stimulated to proliferate as described in "Methods" and incubated with or without 1 μM pirtobrutinib with proliferation analyzed by flow cytometry. Data in panels G-J represent mean from 3 technical replicates. Graphs generated using GraphPad Prism software version 9.3. Analysis of variance and paired *t* test were used to calculate significance. $^{*}P \leq .05$ and $^{**}P \leq .01$. Prog, progression; resp, responding.

Table 1. Time points and genetic characteristics of patients with CLL and disease progression

Patient-identifying code	Time point*	Sample ID	Drug	Days from Dx	WBC count	Absolute lymphocyte count	BTK mutations, CCF (%) (whole-exome sequencing)	BTK mutations, VAF (%) (RNA)
CLL Pt 6		CLL Pt 6 #1	Pretreatment	97	139.6	Not available	No BTK mutation detected	No BTK mutation detected
		CLL Pt 6 #2	After BR+L, before Acala	868	181.45	163.31	No BTK mutation detected	No BTK mutation detected
		CLL Pt 6 #3	Acala	1184	64.46	59.95	No BTK mutation detected	No BTK mutation detected
		CLL Pt 6 #4	Acala	1533	19.48	14.81	No BTK mutation detected	No BTK mutation detected
		CLL Pt 6 #5	Acala	1878	21.42	16.06	p.C481S, 16	p.C481S, 8
		CLL Pt 6 #6	Acala	2037	20.14	13.89	p.C481S, 47; p.T474I, 3	p.C481S, 64; p.T474I, 2
		CLL Pt 6 #7	Acala	2212	51.4	40.61	p.C481S, 92; p.T474I, 4	
		CLL Pt 6 #8	Veca	2261	102.61	96.46	p.C481S, 100; p.T474I, 9	p.C481S, 93; p.T474I, 3
		CLL Pt 6 #9	Veca	2345	237.38	227.88	p.C481S, 93; p.T474I, 3	p.C481S, 91; p.T474I, 2
		CLL Pt 6 #10	Veca	2429	356.2	338.39	p.C481S, 97; p.T474I, 2	p.C481S, 91; p.T474I, 2
		CLL Pt 6 #11	Veca	2492	359.32	341.36	p.C481S, 97; p.T474I, 3	p.C481S, 86; p.T474I, 6
	D 0	CLL Pt 6 #12	Pirto	2599	363.47	341.66	p.C481S, 95; p.T474I, 5	p.C481S, 87; p.T474I, 7
	3 mo	CLL Pt 6 #13	Pirto	2681	148.37	139.47	p.C481S, 69; p.T474I, 24	p.C481S, 40; p.T474I, 32
	6 mo	CLL Pt 6 #14	Pirto	2765	74.81	65.08	p.C481S, 31; p.T474I, 62; p.T474L, 3	p.C481S, 12; p.T474I, 71; p.T474L, 2
	9 mo	CLL Pt 6 #15	Pirto	2856	61.58	54.81	p.C481S, 6; p.T474I, 89; p.T474L, 4; p.M477I, 2	p.C481S, <1; p.T474I, 85; p.T474L, 6
	12 mo	CLL Pt 6 #16	Pirto	2941	105.72	97.26	p.C481S, 2; p.T474I, 99; p.T474L, 5; p.M477I, 2	p.C481S, <1; p.T474I, 87; p.T474L, 8
CLL Pt 7		CLL Pt 7 #1	After FCR	2109	9.5	4.93	No BTK mutation detected	
		CLL Pt 7 #2	Ibr	3266	4.48	2.52	No BTK mutation detected	
		CLL Pt 7 #3	Ibr	4484	21.32	17.51	p.C481S, 6; p.C481R, 33	p.C481S, 7; p.C481R, 18
		CLL Pt 7 #4	Ibr after progression	4532	70.97	38.32	p.C481S, 11; p.C481R, 34	p.C481S, 14; p.C481R, 40
		CLL Pt 7 #5	KTE-X19 CAR-T therapy	4800	12.86	8.33	p.C481S, 16; p.C481R, 31; p.L528W, 1	p.C481S, 25; p.C481R, 24; p.L528W, 2
		CLL Pt 7 #6	KTE-X19 CAR-T	4813	27.53	23.18	p.C481S, 4; p.C481R, 29; p.L528W, 1	p.C481S, 21; p.C481R, 27; p.L528W, 2
	D 0	CLL Pt 7 #7	Pirto	4918	26.71	21.9	p.C481S, 18; p.C481R, 25; p.L528W, 2	p.C481S, 23; p.C481R, 51
	3 mo	CLL Pt 7 #8	Pirto	5009	54.04	50.69	p.C481S, 37; p.C481R, 28; p.L528W, 4	p.C481S, 22; p.C481R, 11; p.L528W, 43
	5.8 mo	CLL Pt 7 #9	Pirto	5094	27.2	19.72	p.C481S, 41; p.C481R, 22; p.L528W, 7	p.C481S, 7; p.C481R, 5; p.L528W, 82
	8 mo	CLL Pt 7 #10	Pirto after progression	5161	30.85	26.99	p.C481S, 28; p.C481R, 20; p.L528W, 30	p.C481S, 5; p.C481R, 2; p.L528W, 91

p.C481S (c.1442G>C); p.C481R (c.1441T>C).
p.T474I (c.1421C>T); p.T474L (two nucleotide changes c.1420A>C; c.1421C>T).
p.M477I (c.1431G>C).
p.L528W (c.1583T>G).
BR + L, bendamustine, rituximab, and lenalidomide; KTE-X19 CAR-T, experimental anti-CD19 chimeric antigen receptor T-cell therapy (Kite); FCR, fludarabine, cyclophosphamide, and rituximab; Veca, vecabrutinib.
*Time point indicates the sample time points (months after pirtobrutinib treatment), which correspond to those used in Figure 4.

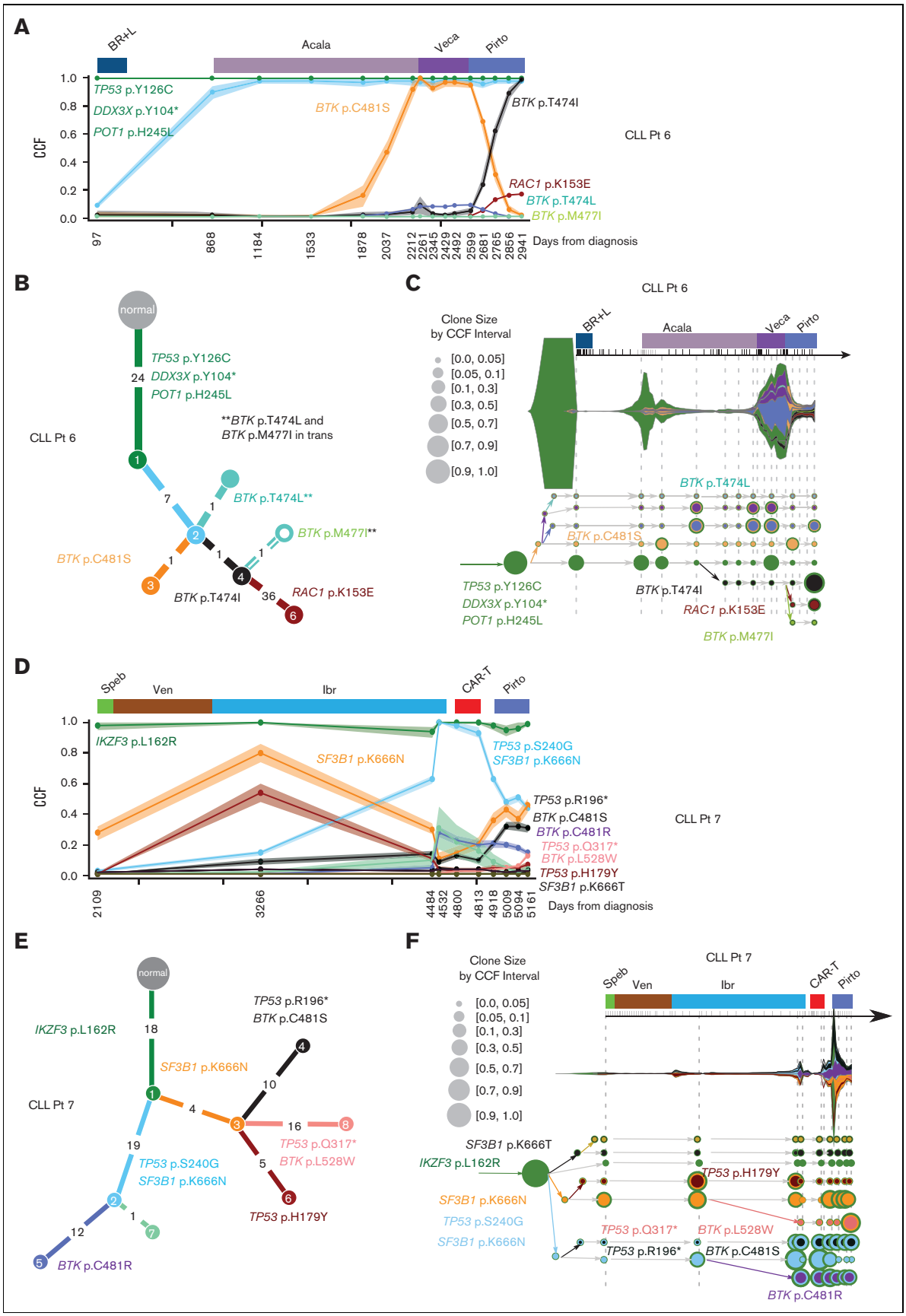

Figure 5.

molecule, thus, bond angles were adjusted and rotated to make it fit into the binding pocket.

BTK gatekeeper mutations T474I and T474L, but not other observed BTK mutations, can activate proximal BCR signaling

To investigate the impact of the mutations on BCR activation, we generated 6 single and 3 double mutants using site-directed mutagenesis and expressed them in the BTK-null DT40 B-cell line. Supplemental Table 7 summarizes the results obtained for the 9 variants and Figure 6B-E depicts representative results. Only T474I, T474L, and C481S mutants showed adequate kinase activity, whereas all the other single or double mutants (M477I, M477I/C481S, M477I/L528W, C481R, L528W, and C481S/L528W) essentially lacked kinase activity as judged by phosphorylation of BTK at Y223[19,20] and PLCγ2 at Y753 (Figure 6B-E; supplemental Table 7). Mutations that lack kinase activity are intrinsically resistant to inhibitors of kinase activity, thus, drug sensitivity could only be assessed for mutations that activate proximal BCR signaling. The C481S variant was resistant to 0.5 μM ibrutinib, as expected, but not to 0.1 μM pirtobrutinib (Figure 6B). Conversely, the T474I and T474L variants were sensitive to 0.5 μM ibrutinib but resistant to 0.1 μM pirtobrutinib (Figure 6E). Interestingly, phosphorylation of AKT and ERK were retained downstream, even with mutations that failed to activate proximal BCR signaling (Figure 6B-E; supplemental Figure 8A-D). Although a slight inhibition of phosphorylation of AKT and ERK was observed in pirtobrutinib-treated cells with the C481S variant, these pathways were not inhibited by ibrutinib or pirtobrutinib in cells expressing any of the other mutations. Furthermore, phosphorylation of AKT and ERK was also observed in the WT B7.10 cell line, which lacks endogenous BTK, demonstrating significant activation of these pathways independent of BTK (Figure 6F).

Discussion

Emergent resistance against covalent BTKis is a growing problem in CLL, from 50% to 75% of patients developing mutation of the target Cys481 residue at the adenosine triphosphate–binding pocket of BTK, thereby abrogating covalent BTKi binding.[1-4] Here, we characterize the activity of the noncovalent BTKi pirtobrutinib against WT and C481S-mutant BTK, using both an in vitro C481S BTK model system and primary CLL cells from patients with CLL. We demonstrate that pirtobrutinib maintains activity against C481S and inhibits the BCR pathway similarly to C481 WT CLL, providing rationale for its study in patients refractory to covalent BTKis, where significant clinical activity, and, in fact, comparable clinical activity, to that seen against C481 WT CLL, has already been demonstrated.[10] Furthermore, we demonstrate that patients responding to pirtobrutinib on clinical trial show sustained inhibition of BCR signaling, whereas patients in whom disease progression had started show reactivation of BCR signaling. This reactivation is associated with the development of multiclonal second-site BTK mutations, many of which lack the ability to activate proximal BCR signaling in a heterologous cell line model. The convergent evolution and oligoclonality of these BTK mutations are striking, and consistent with prior observations with BTK mutations occurring during therapy with covalent inhibitors. Also striking is the reactivation of phosphorylation of AKT and ERK further downstream of the BCR, even in the absence of proximal signaling and indeed in the absence of BTK in a heterologous cell line.

Consistent with a recent report,[32] our data show that pirtobrutinib inhibits BCR signaling downstream of both WT and C481S CLL in a heterologous cell line model and in patient cells.[32] Although Aslan et al[32] observed no clear difference in response between pirtobrutinib and ibrutinib, in vitro incubations of CLL C481S cells in this study demonstrated a noticeably greater sensitivity to pirtobrutinib compared with ibrutinib or acalabrutinib, an observation that is likely attributable to the high C481S VAFs in samples in this study compared with samples in the aforementioned study.[32] In cells of patients with CLL, pirtobrutinib significantly reduces secretion of CCL3 and CCL4 in vitro, regardless of C481S. Similarly, CLL cells from patients responding to pirtobrutinib on the clinical trial show inhibited BCR signaling and cytokine secretion and proliferation in vitro. The increase in phospho-BTK and phospho-ERK observed after 2 cycles of therapy in some responding patients is consistent with recently published data, which showed that the initial decrease in BCR signaling in CLL cells from patients after pirtobrutinib treatment was reversed after 2 cycles of therapy.[32] Our analysis, however, shows that prolonged treatment up to 14 months in responding patients leads to an overall decrease in BCR signaling. At time of progression, however, we see reactivated phospho-BTK, phospho-ERK, and phospho-AKT as well as decreased cellular responsiveness to pirtobrutinib treatment in vitro, as measured by inhibition of proliferation, induction of apoptosis, and secretion of CCL3 and CCL4.

We evaluated the genetic mechanisms of resistance in 2 patients whose disease initially responded but then progressed on pirtobrutinib. Our data provide clinical evidence that gatekeeper and alternative-site BTK mutations lead to resistance to noncovalent BTKis, similar to a recent report.[16] The *BTK* gatekeeper mutation p.T474I identified in a patient with CLL (CLL Pt 6) showed strong clonal selection during pirtobrutinib therapy, effectively replacing the prior C481S clone and demonstrating that mutation of this gatekeeper residue leads to clinical resistance to this noncovalent inhibitor. This rapid selection contrasts with the findings during treatment with vecabrutinib, a noncovalent BTKi with lesser clinical activity, when the p.C481S mutation remained largely unchanged. During pirtobrutinib therapy, the same clone that contains p.T474I

Figure 5. BTK gatekeeper and alternate-site mutation selected during pirtobrutinib therapy for CLL. (A-F) Subclonal structure and clonal evolution of somatic mutations for 2 patients with CLL (CLL Pt 6 and CLL Pt 7) that progressed on pirtobrutinib derived using PhylogicNDT and Concerti. (A,D) Clonal evolution of somatic mutations derived using PhylogicNDT for 2 patients (CLL Pt 6 and CLL Pt 7). Each line represents the CCF distribution dynamics of mutation clusters, generated using the PhylogicNDT Cluster tool, at different time points. Shading represents the 95% confidence interval. (B,E) Phylogenetic tree (built by the PhylogicNDT BuildTree tool) represents the clonal and subclonal architecture. (C,F) Time-scaled Concerti fish plot and tumor evolution tree where width of the fish plot corresponds to absolute lymphocyte counts for the 2 patients (CLL Pt 6 and CLL Pt 7). Clones are sized proportionally to their prevalence and the tree is aligned by sample time point. Subclones are matched in color across the panels for each patient. Speb, spebrutinib; Ven, venetoclax.

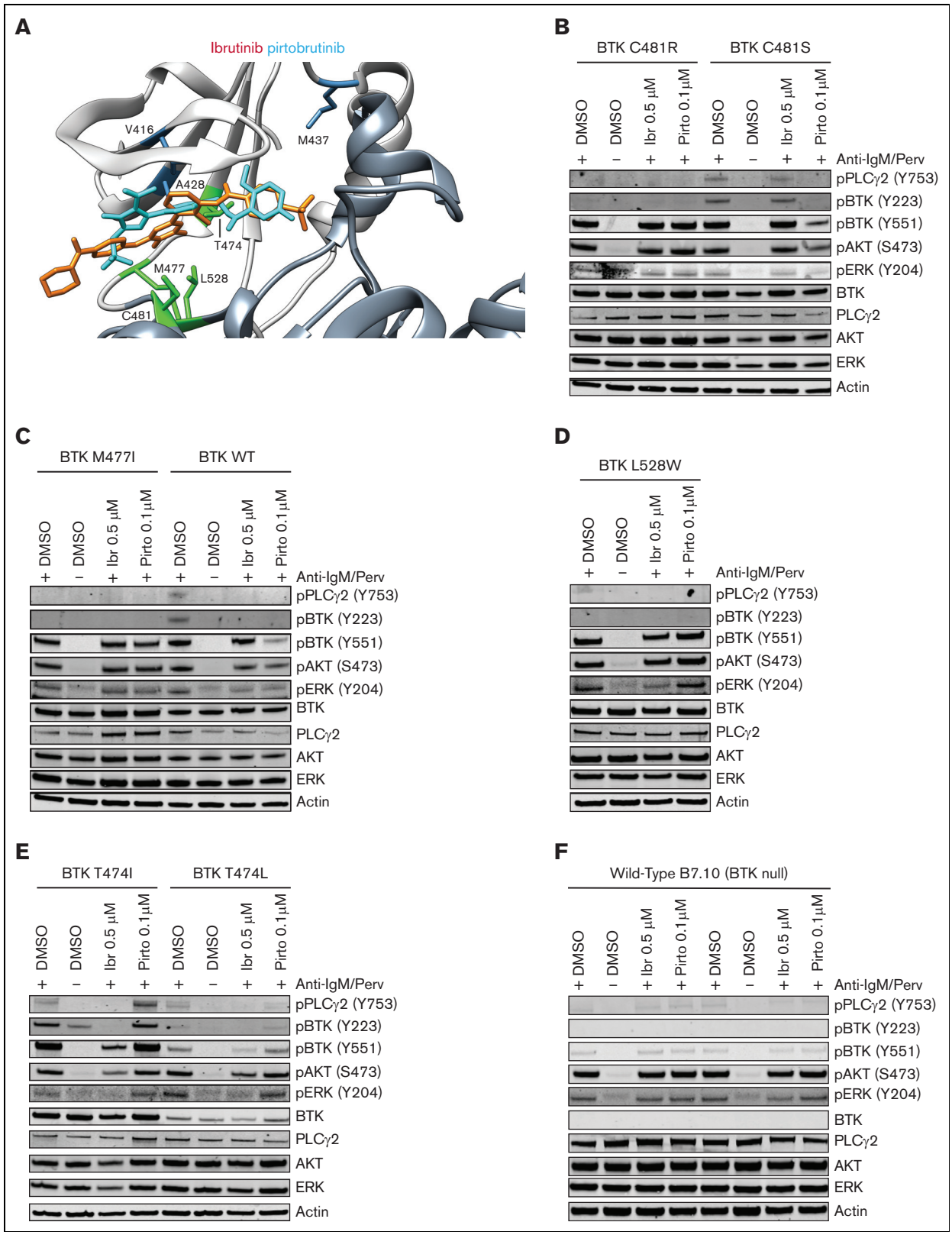

Figure 6. BTK gatekeeper mutations T474I and T474L, but not other observed BTK mutations, can activate proximal BCR signaling. (A) Model of human BTK kinase domain binding modes of covalent inhibitor ibrutinib (orange) and noncovalent inhibitor pirtobrutinib (cyan). Upper domain is in light gray and lower domain is in dark gray. (B-E) B7.10 cells (DT40 cells lacking endogenous BTK) were transfected with BTK C481R, BTK M477I, BTK L528W, T474I BTK, T474L BTK, or C481S BTK, or WT BTK as a control. Cells were starved in medium not supplemented with serum 36 hours after transfection, and treated with 0.1 μM pirtobrutinib for 2.5 hours, or 0.5 μM ibrutinib or DMSO

also harbors a novel previously undescribed BTK mutation identified as p.M477I that is present at very low CCF (2%) in the same cells as p.T474I, and that we show to be inactivating and is only acquired at progression on pirtobrutinib. Furthermore, we observed convergent evolution affecting p.T474, with a subclone containing a p.T474L mutation, a novel mutation we, to the best of our knowledge, report clinically for the first time, and which leads to an active kinase, similar to T474I. This mutation is present at very low CCF but was confirmed by manual review using 3 orthogonal methods (supplemental Figures 6, 7, and 9). The clinical significance of multiclonal BTK mutations at very low CCF remains to be determined but is common in patients who are progressing on covalent BTKis, and suggests strong selection pressure leading to convergent evolution. The predominance of 2 T474 mutations that retain BTK activity in this patient suggest that the mechanism of resistance here is associated with reactivation of the proximal BCR.

The *BTK* p.L528W mutation selected in 1 patient with CLL (CLL Pt 7) during pirtobrutinib therapy has previously been reported at a low CCF of 8% in a patient relapsing on ibrutinib, in patients on zanubrutinib at progression (median VAF, 35%), and recently in 4 patients who progressed on pirtobrutinib.[16,33,34] Computational structural modeling has shown that the p.L528W mutation causes steric hindrance and interferes with the binding of the covalent inhibitors ibrutinib and zanubrutinib to BTK.[16,35] Functional characterization of this mutation by us and by Wang et al[16] demonstrates that this mutation inactivates BTK. We also see a p.C481R clone persisting at a similar VAF at time of resistance; this mutation is also inactivating. In a patient with CLL (CLL Pt 7), a third clone carrying *BTK* p.C481S was observed at progression, which is unexpected because pirtobrutinib maintains activity against *BTK* p.C481S.[36,37] Inspection of variants on IGV shows that p.L528W and p.C481S do not appear on the same sequencing reads (supplemental Figure 10A-B), indicating that they are not in the same clone. The increase in the clone carrying *BTK* p.C481S could be driven by another mutation, in particular the *TP53* p.R196* mutation (supplemental Table 2). In this patient, we saw striking multiclonality of *TP53* mutations increasing over time, consistent with clinical data that TP53 aberrancy also contributes to BTKi resistance.[38] Despite the predominance of the inactivating mutations p.L528W and p.C481R in this patient, and similar to the findings by Wang et al,[16] the patient (CLL Pt 7) showed evidence of intact and increased distal BCR signaling with elevated phosphorylation of AKT and ERK, suggesting an alternative mechanism of activation, perhaps related to proximal bypass of BTK or the scaffolding functions of BTK. Although very few patients have progressed on pirtobrutinib to date, the identification of kinase-dead BTK mutations suggests a novel mechanism of resistance that needs to be elucidated to improve future therapeutic strategies in CLL.[20] Previous work has demonstrated that the SRC family kinase HCK can induce BTK, phosphatidylinositol 3-kinase/AKT, and MAPK/ERK signaling.[39] Furthermore, kinase-dead *BTK* p.C481F/Y mutants have been reported to activate BCR signaling by uniquely recruiting HCK and forming BTK/HCK heterodimers leading to phosphorylation of PLCγ2 and downstream BCR signaling.[40] Rationale therefore exists to determine whether a similar mechanism is operative with the *BTK* mutants p.L528W and p.M477I and this is currently under investigation.

In summary, we show that pirtobrutinib is a potent BTKi in vitro and in vivo, regardless of mutations at C481, with novel multiclonal second-site BTK mutations leading to resistance among patients with preexisting BTK C481 mutations. Interestingly, many of the second-site BTK mutations fail to activate BTK phosphorylation but are still associated with downstream activation of pAKT and pERK; the mechanism of this activation remains to be elucidated. Furthermore, these mutations have occurred predominantly among patients with preexisting C481X mutations; whether patients naïve to covalent BTKis, or those exposed but without preexisting BTK mutations, will demonstrate similar mechanisms of resistance remains to be determined.

Acknowledgments

The authors thank the patients and their families who participated in the pirtobrutinib clinical trial and who were willing to donate samples for this study, Loxo Oncology for providing the authors with pirtobrutinib and HEK293 BTK WT / BTK C481S–transfected cell lines, and the chronic lymphocytic leukemia group at The Ohio State University for gifting the authors with the novel chronic lymphocytic leukemia cell line, OSU-CLL. The authors also thank Karin E. Lundin at the Karolinska Institutet for skillful technical assistance.

This work was supported by a grant from the National Cancer Institute, National Institutes of Health (R01 CA 213442) (J.R.B.), Loxo Oncology (J.R.B.), Broad/IBM Cancer Resistance Research Project (G.G. and L.P.), Cancerfonden and the Center for Medical Innovation, Region Stockholm (C.I.E.S. and R.Z.), and Cancerfonden and Vetenskaprådet (M.V.).

Authorship

Contribution: J.R.B., G.G., I.L., F.U., C.I.E.S., R.Z., M.V., and A.N. designed the research; A.N., I.L., F.U., Q.W., S.M., J.A.L., and J.C. performed research and collected data; J.R.B., J.A.L., I.L., G.G., L.P., K.R., C.L., M.S.D., C.I.E.S., R.Z., and M.V. contributed vital new reagents and analytical tools; J.R.B., I.L., A.N., F.U., Q.W., J.C., M.V., G.S., A.S.K., Y.Z., Y.R., and S.T. analyzed and interpreted the data and performed statistical analyses; A.N., F.U., Q.W., M.V., C.I.E.S., R.Z., and J.R.B. wrote the manuscript; S.M.F., B.P.D., K.S., and R.A.J. provided administrative support (ie, biobanking, managing, and organizing samples); and J.R.B. supervised the study.

Conflict-of-interest disclosure: F.U., K.R., C.L., and L.P. are listed as coinventors of US patent 11189361, a patent related to Concerti. I.L. serves as a consultant for PACT Pharma Inc. and has stock, is on the board, and serves as a consultant for ennov1 LLC., is on the board and holds equity in Nord Bio, Inc. A.S.K. has served as a consultant for LabCorp Inc. and receives research funding from the Multiple Myeloma Research Foundation. M.S.D. has

Figure 6 (continued) for 1 hour. Subsequently, the samples were washed with medium not supplemented with serum 3 times and activated with medium containing pervanadate and mouse antichicken IgM. Representative western blots are shown in panels B-E. Quantification of phospho-BTK, phospho-PLCγ2, phospho-AKT, and phospho-ERK is in supplemental Figure 8. (F) Untransfected (WT B7.10) cells were treated with the indicated doses of the drugs for 1 hour and activated with pervanadate and mouse antichicken IgM–containing medium. Results from duplicate experiments are shown in panel F.

served as a consultant for AbbVie, Adaptive Biotechnologies, Ascentage Pharma, AstraZeneca, BeiGene, Bristol Myers Squibb, Celgene, Eli Lilly, Genentech, Janssen, MEI Pharma, Pharmacyclics, Research to Practice, Takeda, TG Therapeutics, Verastem, and Zentalis and receives research support from AbbVie, Ascentage Pharma, AstraZeneca, Genentech, MEI Pharma, Novartis, Pharmacyclics, Surface Oncology, TG Therapeutics, and Verastem. G.G. receives research funds from IBM and Pharmacyclics; is an inventor on patent applications related to MSMuTect, MSMutSig, POLYSOLVER, and TensorQTL; is also a founder, consultant, and holds privately held equity in Scorpion Therapeutics. J.A.L. consults for Alloplex Biotherapeutics. J.R.B. has served as a consultant for AbbVie, Acerta/AstraZeneca, BeiGene, Bristol Myers Squibb/Juno/Celgene, Catapult, Dynamo, Eli Lilly, Genentech/Roche, Hutchmed, Janssen, Kite, Loxo, MEI Pharma, Morphosys AG, Nextcea, Novartis, Octapharma, Pfizer, Pharmacyclics, Rigel, TG Therapeutics, and Verastem; received honoraria from Janssen; received research funding from Gilead, Loxo/Lilly, Sun, Verastem/SecuraBio, and TG Therapeutics; and served on data safety monitoring committees for Invectys and Morphosys. The remaining authors declare no competing financial interests.

ORCID profiles: F.U., 0000-0003-3226-7642; Y.Z., 0000-0001-6276-635X; S.T., 0000-0002-3119-6507; A.S.K., 0000-0002-8699-2439; G.S., 0000-0001-6630-7935; K.R., 0000-0002-1567-9090; R.Z., 0000-0001-8327-846X; C.I.E.S., 0000-0003-1907-3392; J.R.B., 0000-0003-2040-4961.

Correspondence: Jennifer R. Brown, Dana-Farber Cancer Institute, 450 Brookline Ave, Boston, MA 02215; email: jennifer_brown@dfci.harvard.edu.

References

1. Lampson BL, Brown JR. Are BTK and PLCG2 mutations necessary and sufficient for ibrutinib resistance in chronic lymphocytic leukemia? *Expet Rev Hematol*. 2018;11(3):185-194.
2. Woyach JA, Ruppert AS, Guinn D, et al. BTK(C481S)-mediated resistance to ibrutinib in chronic lymphocytic leukemia. *J Clin Oncol*. 2017;35(13):1437-1443.
3. Woyach JA, Furman RR, Liu TM, et al. Resistance mechanisms for the Bruton's tyrosine kinase inhibitor ibrutinib. *N Engl J Med*. 2014;370(24):2286-2294.
4. Furman RR, Cheng S, Lu P, et al. Ibrutinib resistance in chronic lymphocytic leukemia. *N Engl J Med*. 2014;370(24):2352-2354.
5. Jones D, Woyach JA, Zhao W, et al. PLCG2 C2 domain mutations co-occur with BTK and PLCG2 resistance mutations in chronic lymphocytic leukemia undergoing ibrutinib treatment. *Leukemia*. 2017;31(7):1645-1647.
6. Byrd JC, Harrington B, O'Brien S, et al. Acalabrutinib (ACP-196) in relapsed chronic lymphocytic leukemia. *N Engl J Med*. 2016;374(4):323-332.
7. Johnson AR, Kohli PB, Katewa A, et al. Battling Btk mutants with noncovalent inhibitors that overcome Cys481 and Thr474 mutations. *ACS Chem Biol*. 2016;11(10):2897-2907.
8. Quinquenel A, Fornecker LM, Letestu R, et al. Prevalence of BTK and PLCG2 mutations in a real-life CLL cohort still on ibrutinib after 3 years: a FILO group study. *Blood*. 2019;134(7):641-644.
9. Woyach J, Stephens DM, Flinn IW, et al. Final results of phase 1, dose escalation study evaluating ARQ 531 in patients with relapsed or refractory B-cell lymphoid malignancies. *Blood*. 2019;134(suppl 1):4298-4298.
10. Mato AR, Shah NN, Jurczak W, et al. Pirtobrutinib in relapsed or refractory B-cell malignancies (BRUIN): a phase 1/2 study. *Lancet*. 2021;397(10277):892-901.
11. Gui F, Jiang J, He Z, et al. A non-covalent inhibitor XMU-MP-3 overrides ibrutinib-resistant Btk(C481S) mutation in B-cell malignancies. *Br J Pharmacol*. 2019;176(23):4491-4509.
12. Zhao X, Huang W, Wang Y, et al. Discovery of novel Bruton's tyrosine kinase (BTK) inhibitors bearing a pyrrolo[2,3-d]pyrimidine scaffold. *Bioorg Med Chem*. 2015;23(4):891-901.
13. Reiff SD, Mantel R, Smith LL, et al. The BTK inhibitor ARQ 531 targets ibrutinib-resistant CLL and Richter transformation. *Cancer Discov*. 2018;8(10):1300-1315.
14. Reiff SD, Muhowski EM, Guinn D, et al. Noncovalent inhibition of C481S Bruton tyrosine kinase by GDC-0853: a new treatment strategy for ibrutinib-resistant CLL. *Blood*. 2018;132(10):1039-1049.
15. Woyach JA, Flinn IW, Awan FT, et al. Preliminary efficacy and safety of MK-1026, a non-covalent inhibitor of wild-type and C481S mutated Bruton tyrosine kinase, in B-cell malignancies: a phase 2 dose expansion study. *Blood*. 2021;138(suppl 1):392.
16. Wang E, Mi X, Thompson MC, et al. Mechanisms of resistance to noncovalent Bruton's tyrosine kinase inhibitors. *N Engl J Med*. 2022;386(8):735-743.
17. Takata M, Kurosaki T. A role for Bruton's tyrosine kinase in B cell antigen receptor-mediated activation of phospholipase C-gamma 2. *J Exp Med*. 1996;184(1):31-40.
18. Nawaz HM, Blomberg KEM, Lindvall JM, Kurosaki T, Smith CIE. Expression profiling of chicken DT40 lymphoma cells indicates clonal selection of knockout and gene reconstituted cells. *Biochem Biophys Res Commun*. 2008;377(2):584-588.
19. Estupinan HY, Wang Q, Berglof A, et al. BTK gatekeeper residue variation combined with cysteine 481 substitution causes super-resistance to irreversible inhibitors acalabrutinib, ibrutinib and zanubrutinib. *Leukemia*. 2021;35(5):1317-1329.

20. Hamasy A, Wang Q, Blomberg KE, et al. Substitution scanning identifies a novel, catalytically active ibrutinib-resistant BTK cysteine 481 to threonine (C481T) variant. *Leukemia*. 2017;31(1):177-185.

21. Carter SL, Cibulskis K, Helman E, et al. Absolute quantification of somatic DNA alterations in human cancer. *Nat Biotechnol*. 2012;30(5):413-421.

22. Kasar S, Kim J, Improgo R, et al. Whole-genome sequencing reveals activation-induced cytidine deaminase signatures during indolent chronic lymphocytic leukaemia evolution. *Nat Commun*. 2015;6:8866.

23. Leshchiner I, Livitz D, Gainor JF, et al. Comprehensive analysis of tumour initiation, spatial and temporal progression under multiple lines of treatment. *bioRxiv*. Preprint posted online 16 February 2019.

24. Utro F, Levovitz C, Rhrissorrakrai K, Parida L. A common methodological phylogenomics framework for intra-patient heteroplasmies to infer SARS-CoV-2 sublineages and tumor clones. *BMC Genom*. 2021;22(suppl 5):518.

25. Honigberg LA, Smith AM, Sirisawad M, et al. The Bruton tyrosine kinase inhibitor PCI-32765 blocks B-cell activation and is efficacious in models of autoimmune disease and B-cell malignancy. *Proc Natl Acad Sci U S A*. 2010;107(29):13075-13080.

26. Woyach J, Huang Y, Rogers K, et al. Resistance to acalabrutinib in CLL is mediated primarily by BTK mutations. *Blood*. 2019;134(suppl 1):504.

27. Burger JA, Quiroga MP, Hartmann E, et al. High-level expression of the T-cell chemokines CCL3 and CCL4 by chronic lymphocytic leukemia B cells in nurselike cell cocultures and after BCR stimulation. *Blood*. 2009;113(13):3050-3058.

28. Ponader S, Chen SS, Buggy JJ, et al. The Bruton tyrosine kinase inhibitor PCI-32765 thwarts chronic lymphocytic leukemia cell survival and tissue homing in vitro and in vivo. *Blood*. 2012;119(5):1182-1189.

29. Allan JN, Pinilla-Ibarz J, Gladstone DE, et al. Phase Ib dose-escalation study of the selective, non-covalent, reversible Bruton's tyrosine kinase inhibitor vecabrutinib in B-cell malignancies. *Haematologica*. 2022;107(4):984-987.

30. Robinson JT, Thorvaldsdottir H, Winckler W, et al. Integrative genomics viewer. *Nat Biotechnol*. 2011;29(1):24-26.

31. Zain R, Vihinen M. Structure-function relationships of covalent and non-covalent BTK inhibitors. *Front Immunol*. 2021;12:694853.

32. Aslan B, Kismali G, Iles LR, et al. Pirtobrutinib inhibits wild-type and mutant Bruton's tyrosine kinase-mediated signaling in chronic lymphocytic leukemia. *Blood Cancer J*. 2022;12(5):80.

33. Maddocks KJ, Ruppert AS, Lozanski G, et al. Etiology of ibrutinib therapy discontinuation and outcomes in patients with chronic lymphocytic leukemia. *JAMA Oncol*. 2015;1(1):80-87.

34. Blombery P, Thompson ER, Lew TE, et al. Enrichment of BTK Leu528Trp mutations in patients with CLL on zanubrutinib: potential for pirtobrutinib cross resistance. *Blood Adv*. 2022;6(20):5589-5592.

35. Blombery P, Tam CS, Yeh PS-H, et al. BTK Leu528Trp - a potential secondary resistance mechanism specific for patients with chronic lymphocytic leukemia treated with the next generation BTK inhibitor zanubrutinib. *Blood*. 2019;134(suppl 1):170.

36. Gomez EB, Isabel L, Rosendahal MS, Rothenberg SM, Andrews SW, Brandhuber BJ. Loxo-305, a highly selective and non-covalent next generation BTK inhibitor, inhibits diverse BTK C481 substitution mutations. *Blood*. 2019;134(suppl 1):4644.

37. Naeem AS, Nguy WI, Tyekucheva S, et al. LOXO-305: targeting C481S Bruton tyrosine kinase in patients with ibrutinib-resistant CLL. *Blood*. 2019; 134(suppl 1), 478-478.

38. Ahn IE, Tian X, Ipe D, et al. Prediction of outcome in patients with chronic lymphocytic leukemia treated with ibrutinib: development and validation of a four-factor prognostic model. *J Clin Oncol*. 2021;39(6):576-585.

39. Yang G, Buhrlage SJ, Tan L, et al. HCK is a survival determinant transactivated by mutated MYD88, and a direct target of ibrutinib. *Blood*. 2016; 127(25):3237-3252.

40. Dhami K, Chakraborty A, Gururaja TL, et al. Kinase-deficient BTK mutants confer ibrutinib resistance through activation of the kinase HCK. *Sci Signal*. 2022;15(736):eabg5216.